Study on the Influencing Factors of Ultimate Bearing Capacity for Tx-joints

Junwu Xia[1,2], Jiahui Qian[1,4] and Xinqiang Xia[3]

[1]State Key Laboratory of Intelligent Construction and Healthy Operation and Maintenance of Deep Underground Engineering, China University of Mining and Technology, Xuzhou, Jiangsu, 221116, China

[2]Jiangsu Collaborative Innovation Center of Building Energy-saving and Construction Technology, Jiangsu Vocational Institute of Architectural Technology, Xuzhou, Jiangsu, 221116, China

[3]Shanghai Huajian Engineering Construction Consulting Co., Ltd, Shanghai 200040, China

[4]Corresponding author's e-mail: qjh_js@163.com

Abstract. Based on the construction of steel structures of Xuzhou Concert Hall, the research on the behavior of TX-joints under the combined action of axial force and bending moment was conducted. Finite element (FE) models were established to investigate the influence of the interaction between in-plane T-type branches and out-plane X-type branches on the ultimate bearing capacity of TX-joints. The analysis was focused on the influence of the geometric effect and the load effect on the ultimate bearing capacity of joints under different β (the branch-to-chord width ratio) and load paths. Through linear regression analyses, the joint reinforcement coefficient under spatial action was obtained. It is shown that the expansion of the joints' plastic zone can be effectively restricted by X-type branches. The compression capacity of joints enhances with the increase of X-type branches' coefficient β. The stiffening effect of the in-plane T-type branch is not significant. The load effect on the ultimate bearing capacity of the joints is often negative. With the increase of the X-type branches' moment, the ultimate compressive capacity of the joints will decrease, while the T-type branches' axial force has little influence on the development of the joints' plastic zone.

Keywords: TX-joints; geometric effect; load effect; ultimate bearing capacity

1 INTRODUCTION

Welded steel tube joints with excellent performance, simple appearance and convenient processing of intersection lines are widely used in large-span structures [1]. At present, the research on plane joints is more mature, and the related design standards are gradually improving [2]. Zhao [3] established a model that can well predict the force-deformation behavior of X-joints. Wang [4] evaluated the effect of the chord preload and geometric configurations on behaviors of T- and Y-joints, and proposed

B. Yuan et al. (eds.), *Proceedings of the 2024 8th International Conference on Civil Architecture and Structural Engineering (ICCASE 2024)*, Atlantis Highlights in Engineering 33,
https://doi.org/10.2991/978-94-6463-449-5_6

corresponding bearing capacity formulas. It is found that the stiffener can make the stress distribution in the node domain more uniform, which can effectively improve the bearing capacity of the joint [5-6].

Compared with plane joints, spatial joints have diverse forms and complex forces, Through the comparative analysis of KK- and K-joints, Wu [7] found that the spatial effect has a significant impact on the bearing capacity of KK-joints. Chang [8] also found that the chord pressure significantly affects the bearing capacity of KK-joints, while the chord tension has a negligible effect. Rao [9] discussed the impact of the chord thickness and member action on the bearing capacity of joints, and proposed a modified formula for the reduction coefficient of bearing capacity.

In summary, the ultimate bearing capacity of spatial joints is different from that of corresponding plane joints due to the interaction between members. Moreover, current standards are mostly designed for the axial bearing capacity of joints, but less related to the bending bearing capacity of joints, so it is necessary to conduct in-depth research on the stress performance and design methods of spatial joints. This paper aims to explore the influence of the spatial effect on the ultimate bearing capacity of TX-joints from the perspectives of the geometric effect and the load effect. Regression analysis was used to obtain the reinforcement coefficient of spatial joints, which can provide reference suggestions for the design of TX-joints.

2 ESTABLISHMENT OF FE MODEL

In modeling, plane four-node plastic finite strain shell elements Shell181 are used, and the mesh refinement is carried out near the intersection line. The boundary conditions are that one end of the chord is considered to be fixed, and the other end is only released with the axial translational degrees of freedom along the chord. The boundary of the T-type branch is released all the rotational degrees of freedom, and only the displacement along the axial direction of the branch is free. Only the X-type branch's translational degrees of freedom is constrained. The FE model is shown in Figure 1. Based on the previous static tests [10], axial loads were applied to the ends of each branch and chord, and the bending moment was applied to the X-branch. The FE results and experimental results are compared in Figure 2. It can be seen that the experimental results of the right branch are more consistent with the FE results, while there are some discrepancies in the left branch. The reasons for the errors may be defects in the weld seam. Overall, the FE model can essentially reflect the working performance of the joints and can be used for subsequent research.

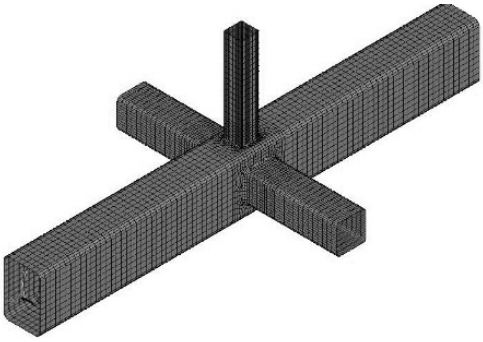

Fig. 1. FE model of the TX-joint.

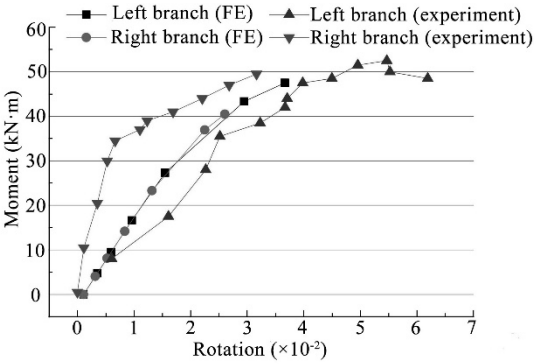

Fig. 2. Comparison of moment-rotation curve.

The previous study has shown that the width ratio β is the focus of the research. Therefore, five groups of different β are selected for modeling. The chord width-to-thickness ratio is 20, and the branch-to-chord thickness ratio is 1. The chord size is 200×300 mm , and the thickness is 10 mm, and the dimensions and parameters of each branch are shown in Table 1, where b1 and t1 indicate branch width and thickness respectively. The TX-joint is a combination of plane joints. For example, the joint T1-X2, which means a spatial joint composed of a plane T-joint T1 and a plane X-joint X2.

Table 1. Size and geometric parameters of joints.

Joint number	Dimension (mm)		Parameter
	b_1	t_1	β
T1	170	10	0.85
T2	160	10	0.8
T3	140	10	0.7
T4	100	10	0.5
T5	80	10	0.4
X1	255	10	0.85
X2	240	10	0.8

X3	210	10	0.7
X4	150	10	0.5
X5	120	10	0.4

3 GEOMETRIC EFFECT ANALYSIS

3.1 Effect of the β_X Value on the Axial Compressive Bearing Capacity of Joints

With the same boundary conditions above, a certain vertical displacement is applied at the end of the T-type branch. According to the method proposed by Lu, the peak load of the joint deformation within the range of 3% b_0 is taken as the ultimate bearing capacity of the joint. If there is no peak load, the load corresponding to the 3% b_0 deformation is taken as the ultimate bearing capacity. As is shown in Figure 3, for the spatial joints with larger β_T, the curves tend to rise slightly in the latter half part, while the corresponding T-type plane joints (β_X=0) have a descending part, which indicates that X-type branches have a reinforcing effect. When β_T is small, the curves are close to each other, indicating that out-plane branches have little effect on the axial elastic stiffness of the joints.

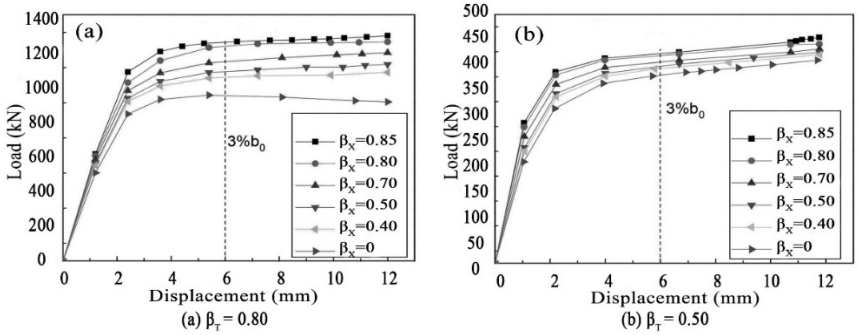

Figure. 3. Load-displacement curve of spatial joints under axial compression.

In Figure 4, the abscissa and the ordinate represent β_X and the ultimate load ratio of spatial joints to the corresponding plane joints (N_S/N_P) respectively. Compared with plane joints, the ultimate bearing capacity of corresponding spatial joints has been improved. The larger the value of β_X, the larger the ultimate bearing capacity of the joints. And the joint T1-X1 has the largest increase of 35.47%.

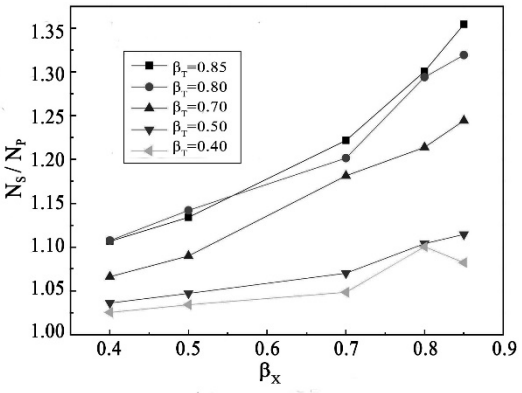

Figure. 4. Influence of geometric effect on ultimate bearing capacity of joints under axial compression.

3.2 Effect of the β_T Value on the Bending Capacity of Joints

In this paper, the depression value is converted into the rotation angle of the joint for defining the ultimate bearing capacity. The boundary conditions are similar to Section 3.1, and a certain rotational displacement is applied to the end of X-type branch. Figure 5 shows that the moment-rotation curve of the spatial joints is similar to that of the corresponding plane joint, showing a slow upward trend without a peak load. In general, the stiffening effect of the T-type branch is not significant, and the elastic rotational stiffness of the joints is basically unchanged.

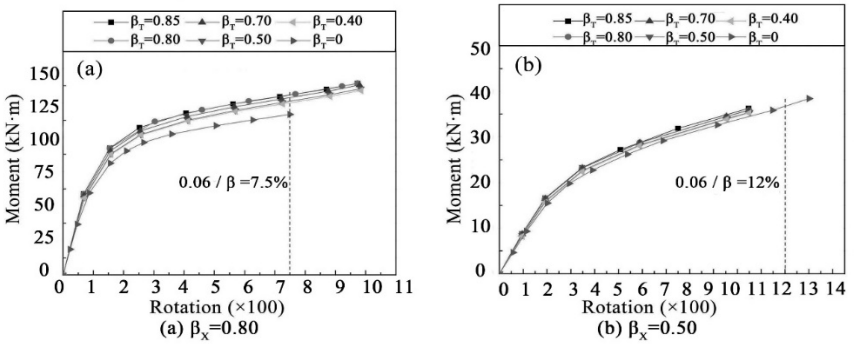

Figure. 5. Moment-rotation curve of spatial joint under moment.

As can be seen from Figure 6, the abscissa and the ordinate represent β_T and the ultimate moment ratio of spatial joints to the corresponding plane joints (M_S/M_P) respectively. The ultimate bending moments of the spatial joints, compared to the corresponding plane joint, are mostly increased, but the increase is not significant. For spatial joints with larger β_X value, the ultimate bending moment increases obviously with the increase of β_T, and the maximum increase is 12.21%.

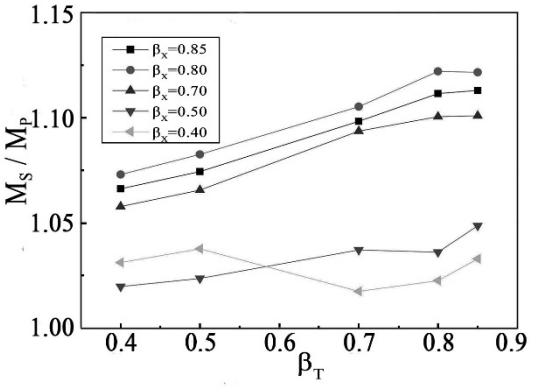

Figure. 6. Influence of geometric effect on ultimate bearing capacity of joints under moment.

3.3 Regression Analysis of the Reinforcement Coefficient

The curve in Figure 4 roughly follows a power function relationship The control parameter is β. The reinforcement coefficient K_1 of the compressive bearing capacity of joints caused by the stiffening of out-plane X-type branches can be written as:

$$K_1 = 1 + C_1(\beta_T)^a(\beta_X)^b \tag{1}$$

With the help of Excel, the data in Figure 4 are analyzed by multiple linear regression with 95% confidence. The FE results are in good agreement with the regression formula, and the maximum error is 2.53%. The final formula of K_1 can be written as:

$$K_1 = 1 + e^{-0.470385}(\beta_T)^{2.128666}(\beta_X)^{1.564565} \tag{2}$$

It can be seen that in-plane T-type branches have little stiffening effect on the spatial joints with smaller β_X value in Figure 6, so the joint data with β_X in the range of 0.7 to 0.85 are selected for multivariate linear analysis. The formula for the reinforcement coefficient K_2 can be written as:

$$K_2 = C_2 + m\beta_T + n\beta_X \tag{3}$$

Using the same method as above, the final formula of K_2 can be written as equation (4). The FE results are in good agreement with the regression formula, and the maximum error is 0.95%.

$$K_2 = 0.952515 + 0.113493\beta_T + 0.085234\beta_X \tag{4}$$

4 LOAD EFFECT ANALYSIS

4.1 Effect of the Out-plane Branch Moment on the Compressive Bearing Capacity of Joints

Different levels of the bending moment are applied to the out-plane X-type branches respectively and remain unchanged, the value of which is 20%, 40%, 60% and 80% ultimate moment of the corresponding spatial joint in Section 3.2. Then the axial force

is applied to the in-plane T-type branch to obtain the corresponding joint's ultimate compressive bearing load, which is defined as $N_{(M/Mu)}$. The spatial joints (T2-X1~T2-X5 and T4-X1~T4-X5) are selected in Figure 7. With the increase of the moment level, the curve shows a significant decrease, which indicates that the out-plane X-type branch bending moment action is unfavorable to the compressive bearing capacity of the joints. When β_T is constant, the effect of bending moment on the compressive bearing capacity of the joint is more obvious as the value of β_X increases.

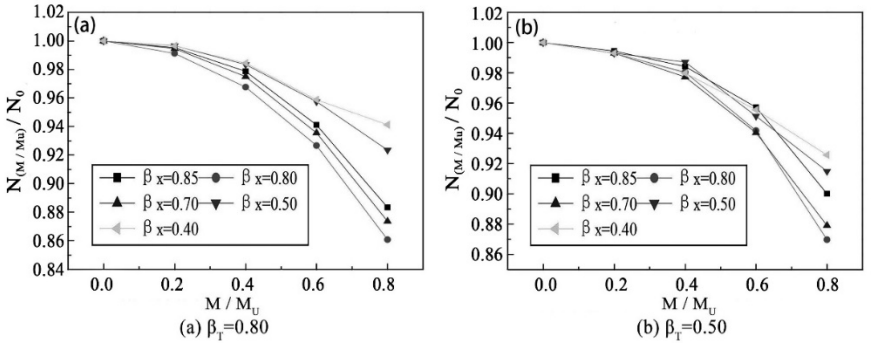

Figure. 7. Influence of out-plane branch moment on compressive bearing capacity of joints.

4.2 Effect of Axial Force of in-Plane Branch on the Bending Capacity of Joints

Different levels of the axial compressive load are applied to the in-plane T-type branches and kept constant, the value of which is 20%, 40%, 60% and 80% corresponding spatial joint's ultimate compressive load in Section 3.1. Then the force couple is applied to the out-plane X-type branch to obtain the corresponding joint's ultimate bending moment, which is defined as $M_{(N/Nu)}$. The spatial joints (X2-T1~X2-T5 and X5-T1~X5-T5) are selected in Figure 8. The curve shows a roughly decreasing trend with the increase of the axial force ratio. For the spatial joints with large β_X, when the axial compression ratio is less than 0.6, the axial force of the in-plane T-type branch has almost no effect on its bending capacity, but when the axial force ratio is 0.8, the bending capacity of the joints decreases significantly. For the spatial joints with small β_X, its bending bearing capacity is sensitive to the axial force, and the maximum decrease reaches 10%.

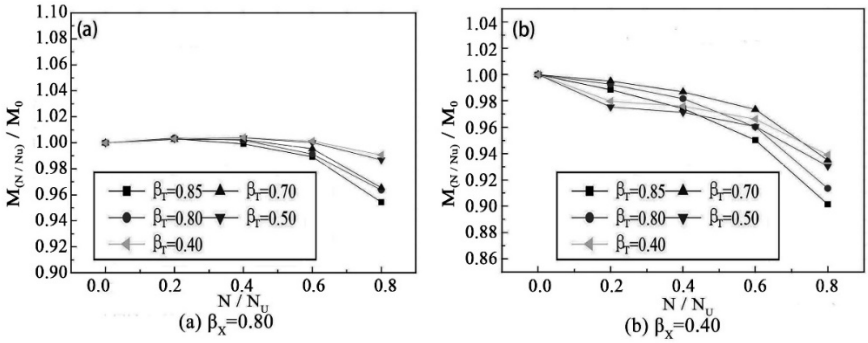

Figure. 8. Influence of in-plane branch axial force on bending capacity of joints.

5 CONCLUSION

(1) The ultimate bearing capacity of spatial joints is closely related to the β value. The higher the value of β is, the more obvious the geometric effect is. The compressive bearing capacity of the joints increases with the increase of β_X, and the ultimate bending moment of the joints increases with the increase of β_T.

(2) Through the method of regression analysis, the formulas for the reinforcement coefficient of the ultimate bearing capacity of the joint under spatial action are obtained, which provides a design basis for the determination of TX-joints' ultimate bearing capacity.

(3) The load effect is unfavorable to the joints. The larger βT is, the more sensitive the compressive bearing capacity of spatial joint is to the out-plane branch bending moment. The axial force of in-plane T-type branch has almost no effect on the bending bearing capacity of spatial joints with larger βX. It is suggested the reduction coefficient of 0.85 should be used in the design. The research on joint stiffness should be strengthened in the future, which affects the stress and deformation of the structure.

ACKNOWLEDGMENTS

The National Natural Science Foundation (52074270); Jiangsu Collaborative Innovation Center for Building Energy Saving and Construction Technology (SJXTZD2106).

REFERENCES

1. Chen, Y., Wang, W., Zhou, F. (2019) Steel tubular structures: configuration innovation and performance improvement driven by new requirements. Journal of Building Structures, 40(3): 1–20. Doi: 10.14006/j.jzjgxb.2019.03.001.

2. Lan, X., Wardenier, J., Packer, J. (2021) Design of chord sidewall failure in RHS joints using steel grades up to S960. Thin-Walled Structures, 163: 107605. Doi: 10.1016/j.tws.2021.107605.
3. Zhao, B., Zheng, J., Liu, C., Saydirakhmono, S., Jiang, Q. Li, K. (2021) Study on the brace axial force-local deformation behavior of unstiffened CHS X-joints. Archive of Applied Mechanics, 91(1): 205-221. Doi: 10.1007/s00419-020-01764-6.
4. Wang, J., Zhang, K., Shu, G., Zheng, B., Jiang, Q. (2021) Investigations on stainless steel T- and Y-joints in cold-rolled circular hollow sections. Journal of Constructional Steel Research, 177: 106462. Doi: 10.1016/j.jcsr.2020.106462.
5. Li, Z., Zhou, F., Wang, W., Xie, W., Ying, T., Yue, G. (2023) Study on static behavior of stiffened CHS tubular welded X-joints. Structural Engineers, 39(2): 87-96. Doi: 10.15935/j.cnki.jggcs.2023.02.010.
6. Guo, X., Xu, Z., Liu, J., Luo, J. (2023) In-plane flexural capacity of eccentric RHS beam-column joints. Journal of Hunan University （Natural Sciences）, 50(01): 45-58. Doi: 10.16339/j.cnki.hdxbzkb.2023005.
7. Wu, Z., Zhang, Z., Ding, Y., Zhang, Y. (2004) Experimental research on static behavior of square hollow section K-and KK-joints. Journal of Building Structures, 25(2): 32–38.
8. Chang, X., Wang, B., Liu, Z., Sun, F., Zhang, Y. (2021) Study on ultimate bearing capacity of KK-type steel tube-sheet joint in drilling derrick space. Modern Mining, 37(10): 167-172.
9. Rao, T., Du, X., Yuan, H., Len, Z., Cao, H. (2022) A study on the load-carrying behavior of full-width KX-shaped RHS joints. Progress in Steel Building Structures, 24(2): 79–87. Doi: 10.13969/j.cnki.cn31-1893.2022.02.008.
10. Xia, J., Xia, X., Chang, H., Hou, Z. (2011) Experimental research on static behavior of TX-type square tube joints under combined load. Journal of Xuzhou Institute of Architectural Technology, 11(1): 1–4.